A Kernel-Based Post-Process for Image Segmentation Using GVF Snake

Saman Ghaffarian
Geomatics Engineering Department, Universityof Hacettepe, Turkey
Email:ghaffarian.saman@gmail.com

***Abstract*—This paper presents a kernel-based post-process for the segmentation of multiple objects using gradient vector flow (GVF) snake (active contour) algorithm. GVF snake has stronger convergence proficiency to boundary convexities and concavities than traditional snake. However, because of the nodes affiliation to each other and mislead of external and internal forces thatare used in GVF snake, some of the nodes remain between trueboundaries as they push toward true boundaries, and resultsin an incorrect segmentation. Our algorithm has two steps. First we decomposedeach pixel of image toits lower size and composed a new image with new grid sizes, then we used an adaptive kernel-based standard deviation calculation for each node of snakes to evaluate its accuracy if it is true segmented result or not. We have tested the proposed method on some sorts of synthetic images and a gray-level real satellite image thatwas captured with Orbview3 panchromatic band with 1m resolution and we have achieved considerable results.**

***Index Terms*—GVF snake, image segmentation, kernel-based, post-process.**

I. Introduction

Image segmentation is one of the first and most important tasks in image analysis and computer vision. Although various methods havebeen proposed in the literature, the design of robust and efficient segmentation algorithms is still a very challenging topic, due to the variety and complexity of images [1], [2].

A snake is defined as an energy minimizing spline guided by external constraint forces and influenced by image forces that pull it toward features such as lines or edges [3], [4]. However, classical parameter snakes are well known to be topologically inflexible. They are incapable of dealing with more complicated object shapes as well as multiple-object scenes [5]. To increase the snakes' topological adaptability, “topology adaptive snakes” or T-snakes havebeen developed as a new class of deformable contour models, by using the affine cell image decomposition (ACID) of an image domain to reparameterize the model during the deformation process. However, this approach may result in convergence failure in many complicated cases and fail in the presence of noise. Moreover to extract the real boundary of the target, the internal and external energy used in deformable contour model should be defined based on the type of images for which it is efficient [5]-[7].

The gradient vector flow (GVF) snakes are dense vector fields derived from images by minimizing energy functional in a variation-based framework. The minimization is achieved by solving a pair of decoupled linear partial differential equations which diffuses the gradient vectors of a gray-level or binary edge map computed from the image [8]. In such a way, if the initial snake is far from true object boundaries, it can also be attracted by the GVF field. The efficiency of gradient diffusion depends on a regularization parameter that must be carefully fine-tuned by users [9].

All implicit snake models often cannot process multiple or annular objects. After getting results from the snake, nodes that may remain in the unwanted regions may cause some inaccurate segmentation results.

This paper presents a post-process approach; by forming adaptive kernels around nodes' cells after composing new cells in new grids. And calculating the standard deviations in mentioned kernels and selecting an appropriate threshold for removing the incorrect nodes on segmentation results.

II. A Brief Glance Through Snakes

A. Traditional snake

Traditional snake is a controlled continuity curve under the influence of internal and external constraint forces [2], [7].

The internal energy $E_{\text{int}}(k(s))$ can be written:

$$E_{\text{int}}(k(s)) = \frac{\alpha(s)|k_s(s)|^2 + \beta(s)|k_{ss}(s)|^2}{2} \quad (1)$$

where $k(s) = (x(s), y(s))$ is the curve of the snake, s is the parameter of the curve and $k_s(s)$, $k_{ss}(s)$ demonstrate the first and second derivatives, respectively. α and β are weighting parameters that control the snake's tension and rigidity, respectively.

The external energy function $E_{ext}(k(s))$ is derived from the image which attracts the snake (curve) to lines, edges and terminations in otherwords; the external energy pushes the snake (curve) toward high or low intensity junctions. The total image energy can be expressed as a

Manuscript received September 9, 2013; revised November 20, 2013.

doi: 10.12720/joace.2.3.277-281

weighted combination of theenergy that is derived from image.

As usual external energies are:

$$E_{ext}(k(s)) = -\left|\nabla I(k(s))\right|^2 \tag{2}$$

$$E_{ext}(k(s)) = -\left|\nabla(G_\sigma(k(s) * I(k(s))\right|^2 \tag{3}$$

where $I(k(s))$ is a gray-level image, $G_\sigma(k(s))$ is a two-dimensional Gaussian function with standard deviation σ and ∇ is the gradient operator. In this definitionitis clear that larger σ 's will occasion the boundaries to become opaque and distorted. However, to use this, the external energy has been minimized. Altogether, the snake model represents a compromise between the internal and external energy status via the weighting parameters.

B. GVF Snake

Gradient vector flow snake is an active contour model which uses vector field $V(k(s)) = (u(k(s)), v(k(s)))$ to minimize the energy function that is computed for any image pixel $k(s) = (x(s), y(s))$:

$$\varepsilon = \iint \mu(p_x^2 + p_y^2 + q_x^2 + q_y^2) + |\nabla f|^2 |V - \nabla f|^2 \, dxdy \tag{4}$$

where ∇f is the gradient of the edge map, f derived from the input image $I(k(s))$, μ is an adjustment parameter, and $dxdy$ indicates partial derivatives with respect to x and y axes. After the minimization process, $V(k(s))$ will be approximately zero where ∇f is larger (wherever the intensity changes significantly). The gradients are dispersed from heterogeneous areas to homogeneous regions.

Each node of the curve has been affected with these vectors and pushed to reach the object boundaries (wherever the intensity changes significantly). After all, these nodes connect to each other and establish the final segmentation result.

III. The Proposed Post-Process Model

This paper establishes a post-process for GVF snakes based on adaptive kernels. Whilst it can be also used to post-process any snake model but it gives more substantial amendment results in GVF snakes.

The GVF snake has problems when used in segmenting complicated shapes with narrow concavities and multi-object images and relies on the initialization.To solve these problems we developed a process that has two main steps, indeed this is a post-process procedure and we implemented these steps after the snake has done. In the first step we decomposed each pixel to 0.1 of the original size of the pixel and filled the cells; this step is a pixel by pixel process that only compartment each pixel to 100 pixels, then we composed the new cells with each other, so we had 10*10 cells for each cell in original image with thesame value of that cell. In this step we just decomposed the pixels and filled them with the equivalent cell values in original image and we did nothing for the image resolution so there was no change in appearance of the image. (Fig. 1).

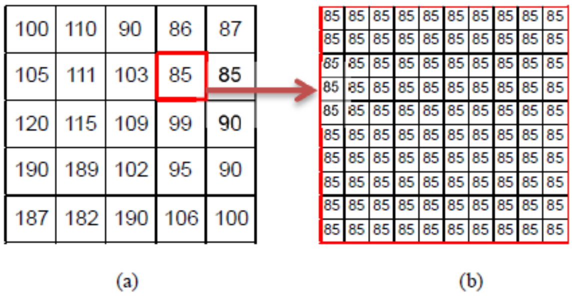

Figure 1. (a) The original image with original grid and cell sizes. (b) The decomposing operation done for a specified cell and has filled values according to the above descriptions.

On the other hand we have n nodes with coordinates of (x, y) that they resulted in an implementation of the snake algorithm on specified image. For using this node's coordinates we should transform this coordinates to our newly composed coordinate system, for this we just multiplied the original coordinates to 10 because we have dividedeach cell into 10 columns with 10 rows cells. (Fig. 2)

In the second step after composing the new grids and transforming the node's coordinates into new grid cell sized image, we constructed a kernel matrix with adaptive sizes of even numbers depending on properties of that image.

We used these kernels where each node of the snake exactly centered in the kernel and selected the pixel values around that node regarding the size of kernel. Then we exerted these brightness values (BVs) to calculate the standard deviation σ of the BVs in the kernel around the node using the equation below.

$$\sigma = \left(\frac{1}{n-1}\sum_{i=1}^{n}(BV_i - \overline{BV})^2\right)^{\frac{1}{2}} \tag{5}$$

where

$$\overline{BV} = \frac{1}{n}\sum_{i=1}^{n} BV_i \tag{6}$$

And n is the number of elements in the kernel.

In the boundaries and features edges the variation and the standard deviation of the BVs are larger than homogenous areas thatare why we used this property to choose and decide if the node is located rightly or not. For this, after calculation of the standard deviation we determined a threshold (A1) and removed the nodes that had not sufficient standard deviation values.

So automatically editing and refining the snake's results that significantly increase the accuracy of the segmentation results became available. (Fig. 3), (Table III).

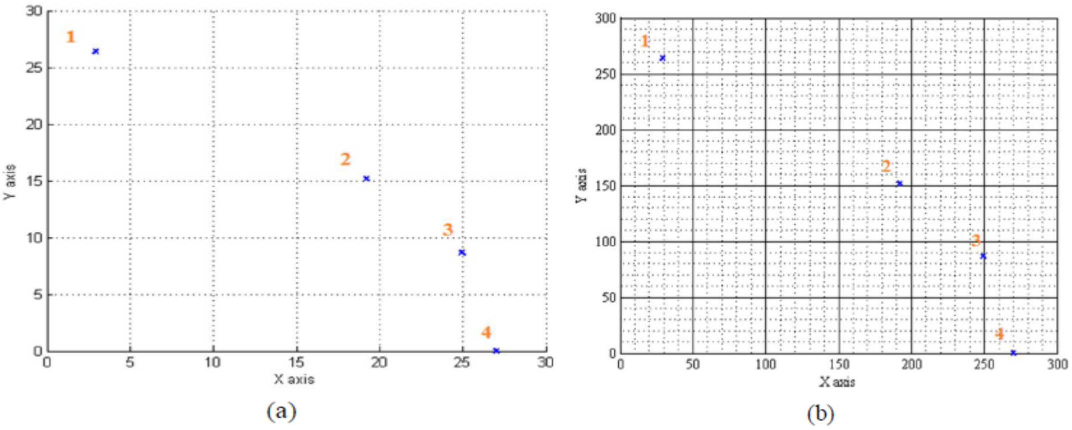

Figure 2. (a) The original image with original grid and cell sizes with original nods coordinates below it in Tabel I. (b) The decomposed operation done for a specified cell and the nods coordinate changes upon on in Tabel II

TABLE I. COORDINATES IN ORIGINAL IMAGE

Node Number	Coordinates	
	x	y
1	27	0
2	24.92	8.63
3	19.19	15.15
4	2.93	26.37

TABEL II. COORDINATES IN NEWLY COMPOSED IMAGE

Node Number	Coordinates	
	x	y
1	270	0
2	249.2	86.3
3	191.9	151.5
4	29.3	263.7

.

255	255	255	255	255	255	0	0	0	0	0	0	0
255	255	255	255	255	255	0	0	0	0	0	0	0
255	255	255	255	255	255	0	0	0	0	0	0	0
255	255	255	255	255	255	0	0	0	0	0	0	0
255	255	255	255	255	255 2	0	0	0	0	0	0	0
255	255	255	255	255	255	0	0	0	0	0	0	0
255	255	255	255	255	255	0	0	0	0	0	0	0
255	255	255	255	255	255	0	0	0	1 0	0	0	0
255	255	255	255	255	255	0	0	0	0	0	0	0
255	255	255	255	255	255	0	0	0	0	0	0	0
255	255	255	255	255	255	0	0	0	0	0	0	0
255	255	255	255	255	255	0	0	0	0	0	0	0
255	255	255	255	255	255	0	0	0	0	0	0	0

Figure 3. Example for conducting kernel around the nodes. This is a binary image with 8 bits ratio.

TABLE III. CALCULATIONS FOR EACH KERNEL

Node Number	Kernel Size	Standard Deviation
1	5x5	0
2	5x5	127.5

Calculations for the example on the Fig. 3.

IV. EXPERIMENTAL RESULTS

In this section, experimental results of the synthetic images obtained with proposed algorithm are presented. All the synthetic images have been chosen especially to show the benefits of this algorithm and its comparison with GVF snake results. Finally we run the program on a real satellite image and analysis the obtained results.

A. *Experimental Results on the Synthetic Images*

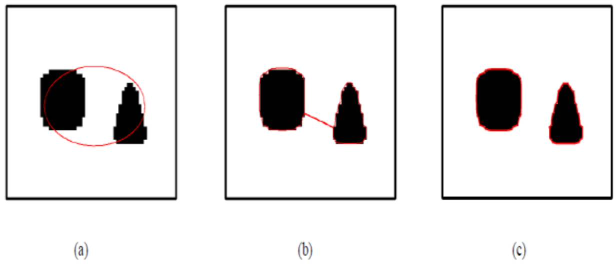

Figure 4. Abinary image including dual-object with different shapes. (a) The initialized image, (b) result of GVF snake with ($\alpha = 0.05$, $\beta = 0$, $\gamma = 1$), (c) final result after refining with our proposed method using 31x31 kernel size and 0.1 threshold for σ .

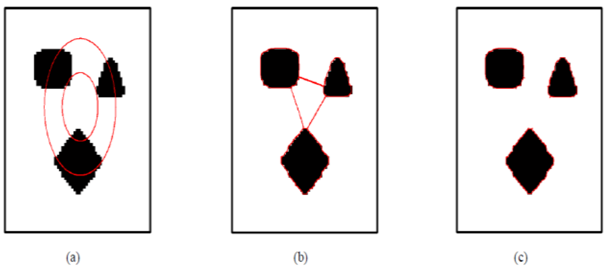

Figure 5. Multi-objected binary image with different shapes. (a) The initialized image, (b) result of GVF snake with ($\alpha = 0.05$, $\beta = 0$, $\gamma = 1$), (c) final result after refining with our proposed method using 41x41 kernel size and 0.1 threshold for σ .

We chose various synthetic images with different properties of convexities, concavities, shape and number of objects that they have involved. Firstly, we show the results in a binary image with two objects and parameters that we used in GVF snake in this image are ($\alpha = 0.05$, $\beta = 0$, $\gamma = 1$). And the kernel size that we used for post process and refined the results in our proposed model in this image is 37x37 and the threshold for standard deviation was under 0.1, it means that every node that have standard deviation in their kernel under 0.1 will be removed.(Fig. 4).

In Fig. 5, we have three objects with different shapes. The GVF snake's parameters that were used in this image are ($\alpha = 0.05$, $\beta = 0$, $\gamma = 1$) and we used 41x41 kernel size and 0.1 threshold for standard deviation σ limitation.

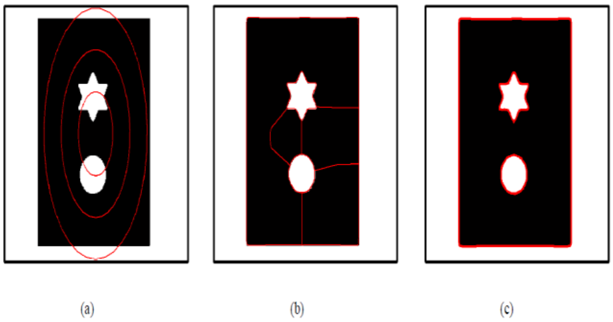

Figure 6. An image with an object including two inner objects with diverse convexity, concavity and shapes. (a) The initialized image , (b) result of GVF snake with ($\alpha = 0.05$, $\beta = 0$, $\gamma = 1$), (c) final result after refining with our proposed method using 41x41 kernel size and 0.1 threshold for σ .

In Fig. 6, an object including two inner objects with diverse convexity, concavity and shapes that is a challenging try for GVF snake whereas it can be corrected with our introduced kernel-based post-process model. Parameters which used for this image are ($\alpha = 0.05$, $\beta = 0$, $\gamma = 1$) in GVF snake and 41x41 kernel size with 0.1 threshold of σ .

The synthetic images which we have chosen to demonstrate the results of our proposed method all are binary images and have two obvious distinguishable brightness values (black and white) accordingly we used a standard deviation threshold below one ($\sigma \leq 0.1$). However, it can differ and be higher in the gray-level images.

B. Experimental result on a satellite image

Finally in Fig. 7, we tested our model on a real satellite image. This image belongs to fish farming ponds in the suburban area of Tabriz city in Iran, which captured with Orbview3 satellite with its panchromatic band and has 1 m resolution.

When we used our model in gray-level images we should be more patient on choosing the kernel size and threshold of standard deviation σ for correct the GVF snake. In the gray-level images, we might have some noises that can impress the standard deviation result. In order to reduce the effect of the noises we have two options in our proposed model, standard deviation threshold and adaptive kernels, which we can use as for image brightness values variations and objects' locations. In Fig. 7c, we can see that by choosing both a right kernel size and threshold of standard deviation we can achieve a perfect segmentation result, in this test we used($\alpha = 0.05$, $\beta = 0$, $\gamma = 1$) for GVF snake parameter and kernel size of 41x41, threshold of $\sigma \leq 11$ for achieving the current result.

V. Conclusion

In this research, a post-process corrigendum has introduced for GVF snake based on adaptive kernels. This post-process models consideration focused on simple statisticalcalculations as well as positions of thenodes of the curves which resulted from snake algorithm and has explained in section III. We proposed two options in our model to correct the GVF snakes results; 1-The kernel sizes around the nodes 2-Threshold on standard deviation of the BVs of the kernels around nodes. We have tested successfully our introduced model in various shaped and multi-objected synthetic images (Fig. 4, Fig. 5, and Fig. 6) and a gray-level real satellite image of fish farming ponds (Fig. 7). It is obvious that this new method can be a good choice for emending and refining any incorrect image segmentation results with defining rigorously the options of the algorithm.

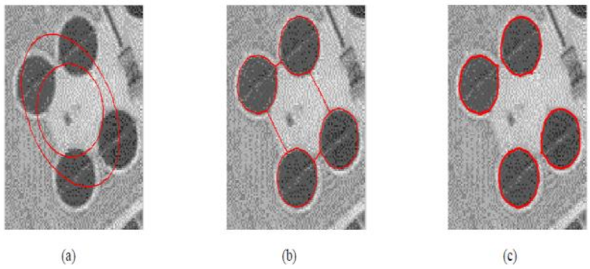

Figure 7. A gray-level image with 1m spatial resolution. (a) The initialized image, (b) result of GVF snake with ($\alpha = 0.05$, $\beta = 0$, $\gamma = 1$), (c) final result after refining with our proposed method using 41x41 kernel size and 11 threshold for σ .

Appendix

A.1. Pseudo-codes (Matlab-codes) for the rule of trammeling the standard deviation σ .

```
Begin Procedure: A. 1
For each node X coordinate, Y coordinate, Kernel size (ker)
and its values given that are resulted from prior computations
sker = std2 (ker (:) ) ;
if sker<= 0.1
    X = NaN ;
    Y = NaN ;
end
End procedure: A.1
```

Acknowledgment

The Orbview3 panchromatic band image was provided from USGS web sites archives (www.earthexplorer.usgs.gov).

References

[1] X. Munoz, J. Freixenet, X. Cufi, and J. Marti, "Strategies for image segmentation combining region and boundary information," *Pattern Recognition Letters*, vol. 24, no. 1, pp. 375-392, Jan 2003.

[2] S. Krinidis and V. Chatzis, "Fazzyenergy-based active contours," *IEEE Trans. Image Processing*, vol. 18, no. 12, pp. 375-392, Dec 2009.

[3] M. Kass, A. Witkin, and D. Terzopoulos, "Snakes: Active contour models," *International Journal of Computer Vision*, vol. 1, no. 4, pp. 321-331, Jan 1987.

[4] M. Kabolizade, H. Ebadi, and S. Ahmadi, "An improved snake model for automatic extraction of buildings from urban aerial images and LiDAR data," *Computers, Environment and Urban Systems*, vol. 34, pp. 435-441, April 2010.

[5] X. F. Diao, X. Y. Zhang, T. F. Wang, S. P. Chen, and L. H. Li, "Robust topology-adaptive snakes for medical ultrasonic image segmentation," in *Proc. BMEI*, 2010, pp. 527-530.

[6] T. McInerney and D. Terzopoulos, "T-snakes: Topology adaptive snakes," *Med. Image Anal.*, vol. 4, pp. 73-91, June 2000.

[7] L. Ji and H. Yan, "Robust topology-adaptive snakes for image segmentation," *Image and Vision Computing*, vol. 20, pp, 147-164, 2002.

[8] C. Xu and J. L. Prince, "Gradient vector flow: A new external force for snakes," in *Proc. Conf. on Comp. Vis. Patt. Recog*, 1997, pp. 66-71.

[9] C. H. Chuang and W. N. Lie, "Automatic multi-object segmentation by two-phase snake processing," *Asian Journal of Health and Information Sciences*, vol. 1, no. 3, pp. 296-320, 2006.

Saman Ghaffarian was born in Tabriz, Iran, in 1985. He received B.S., degree in civil engineering, from Azad University of Tabriz, in 2008. Presently he is pursuing his M.S. in Geomatics engineering, in Hacettepe University, Ankara, Turkey. His interested areas are Satellite Image Processing and Analysis, Image Processing, Automatic Detection of Agricultural parcel boundaries Satellite Images, Object-Based Image Segmentation and Classification.